

Altering the Context of an RNA Bulge Switches the Binding Specificities of Two Viral Tat Proteins[†]

Colin A. Smith, Shane Crotty, Yoko Harada, and Alan D. Frankel*

Department of Biochemistry and Biophysics, University of California, San Francisco, San Francisco, California 94143-0448

Received February 18, 1998; Revised Manuscript Received May 27, 1998

ABSTRACT: The bovine immunodeficiency virus (BIV) Tat protein binds with high affinity to its TAR RNA site through a large set of specific RNA–protein contacts whereas human immunodeficiency virus (HIV) Tat makes relatively few contacts to HIV TAR and requires the assistance of a cellular protein to bind with high affinity. The two TAR sites are structurally very similar, but BIV Tat appears unable to make the same set of high-affinity contacts to HIV TAR. To determine the basis of this discrimination, we examined BIV Tat binding to a series of hybrid TARs both *in vivo* and *in vitro*. We expected that differences in the architectures of the bulges might account for the binding specificity; however, the results show that flanking base pairs provide the key determinants. Based on these data, we designed a novel TAR that is recognized by both BIV Tat and HIV Tat. This RNA may be viewed as a primordial TAR from which two distinct recognition strategies can be evolved.

Studies of small RNA–peptide model systems have revealed a variety of structural solutions to the problem of RNA–protein recognition. Arginine-rich peptides from human immunodeficiency virus (HIV) Rev and bacteriophage λ N proteins recognize internal and terminal RNA loops using α -helical conformations, a bovine immunodeficiency virus (BIV) Tat peptide recognizes an RNA bulge using a β -hairpin conformation, and an HIV Tat peptide recognizes an RNA bulge using an apparently extended conformation (1–8). The BIV and HIV Tat–TAR complexes provide particularly interesting examples of how two closely related RNA sites can be recognized using very different binding strategies. Besides differences in peptide conformation, these two complexes are composed of markedly different RNA–protein contacts, and HIV Tat binding is assisted by an additional cellular protein. Both Tat proteins are essential for viral replication and activate transcription by binding to the TAR sites located at the 5' ends of the viral transcripts; thus, it is interesting to consider how such different RNA-binding strategies evolved in the two closely related systems.

In HIV Tat, a single arginine residue within the arginine-rich domain is largely responsible for recognition of TAR, with surrounding basic amino acids helping to raise the RNA-binding affinity and specificity (9, 10). An NMR model of a TAR–argininamide complex, which mimics the RNA–peptide interaction, suggests that the critical arginine residue hydrogen bonds to G26 and contacts two important phosphates (11). TAR undergoes a large conformational change upon binding in which U23 of the bulge forms a base triple with the A:U base pair just above G26, helping to correctly position the phosphates and stabilize the complex. In contrast to the relatively well-ordered TAR structure, it is less clear whether the Tat peptide adopts a defined confor-

mation either upon RNA binding or in the context of the full-length protein (2, 3, 12). Transcriptional activation by HIV Tat appears to require an accessory protein, most likely cyclin T, that binds to the TAR loop and increases the affinity and/or stability of the Tat–TAR complex *in vivo* (13–15). The existence of the protein has been inferred from the loop sequence requirements, which are not important for Tat binding, and from the observation that weak activity in murine cells can be strengthened in a loop-dependent manner by supplying human chromosome 12, which appears to encode the factor. The spacings between the TAR bulge and loop, and between the Tat arginine-rich and activation domains, must be maintained for high activity (10, 16, 17), consistent with a model in which the loop-binding protein contacts both the TAR loop and the Tat activation domain, thereby increasing the affinity of the complex. RNA binding by the accessory protein does not appear to be required for Tat activation because replacing TAR and the Tat arginine-rich domain with other RNA–protein interactions, such as the R17 coat protein–RNA interaction, supports efficient Tat function both in human and in murine cells (18, 19). Nevertheless, the cellular protein still may be recruited into the transcription complex in the absence of TAR through interactions with Tat.

In contrast to the HIV case, the arginine-rich domain of BIV Tat binds with high affinity to BIV TAR and does not require the assistance of a host protein. Biochemical experiments have shown that eight amino acids in the arginine-rich domain (three arginines, three glycines, one threonine, and one isoleucine) and two G:C base pairs, an additional G nucleotide, and one bulge nucleotide in BIV TAR are essential for binding (20, 21). NMR experiments have shown that the BIV peptide adopts a β -hairpin conformation and binds deeply within the TAR major groove, and a base triple analogous to that in HIV TAR is formed (4, 5). Contacts between all essential amino acids and bases

[†] Supported by NIH Grant AI29135 and by an ACS postdoctoral fellowship (C.A.S.).

are observed, though the role of one arginine is unclear. Notably, Arg73 binds to G11 in an arrangement strikingly similar to that of the HIV TAR–arginine interaction.

Despite the different binding strategies, the secondary and tertiary structures of the HIV and BIV TAR sites are highly related, and it was expected that the BIV peptide would be capable of binding HIV TAR with high affinity and in the same manner as to its own site. However, the BIV peptide binds HIV TAR only weakly *in vitro*, and a fusion protein between the BIV Tat arginine-rich domain and the HIV Tat activation domain poorly activates an HIV TAR reporter (20). The fusion was not expected to function using the loop-dependent HIV strategy because the BIV RNA-binding domain lacks necessary basic residues flanking the arginine analogous to that in HIV Tat (10). To explore why BIV Tat discriminates against HIV TAR despite its similarity to BIV TAR, we analyzed BIV Tat activities *in vitro* and *in vivo* using a series of hybrid and mutant TARs. The results indicate that a base pair adjacent to the loop, and base pairs in the lower stem, account for the binding difference. Based on these results, we constructed a TAR variant that is highly activated by both HIV and BIV Tat, suggesting a simple path for the evolution of TAR sites with distinct HIV and BIV recognition strategies.

MATERIALS AND METHODS

Comparison of NMR Models. Average NMR models of the BIV TAR–peptide complex (4) and TAR–argininamide complex (11) were superimposed using InsightII software (Biosym Technologies) to maximize the overlap (based on rms deviation) of the following bases: BIV G11 and HIV G26; BIV A13 and HIV A27; BIV G14 and HIV G28; BIV G22 and HIV G36; BIV C23 and HIV C37; BIV U24 and HIV U38; BIV C25 and HIV C39.

Peptide Synthesis, Purification, and Analysis. BIV Tat_{65–81} peptide was synthesized on an Applied Biosystems Model 432A peptide synthesizer using Fmoc chemistry and standard resin (25 μ mol) and protecting groups, as previously described (20). The N-terminus was acetylated using acetic acid (75 μ mol) with HBTU activation. Following cleavage and deprotection in the presence of reagent R, peptides were purified on a C₄ reverse-phase HPLC column (Vydac) using an acetonitrile gradient of 0.2%/min in 0.1% trifluoroacetic acid. Purity and concentration were determined by electrospray mass spectroscopy and amino acid analysis (University of Michigan Protein and Carbohydrate Structure Facility).

RNA Synthesis and Purification. Wild-type and mutant TAR RNAs were transcribed by T7 RNA polymerase using synthetic oligonucleotide templates (22). All RNAs contained GG at the 5' end, which increases the efficiency of transcription, and CC at the 3' end to base pair with the Gs. For randomly labeled RNAs, [α -³²P]CTP (3000 Ci/mmol) was included in the transcription reaction. RNAs were purified on 20% polyacrylamide/8 M urea gels, eluted from the gels in 0.6 M NaOAc, pH 6.0, 1 mM EDTA, and 0.01% SDS, and ethanol precipitated twice. Purified RNAs were resuspended in sterile deionized water. The concentrations of radiolabeled RNAs were determined from the specific activity of [³²P]CTP incorporated into the transcripts. RNAs were renatured by incubating in renaturation buffer (10 mM Tris-HCl, pH 7.5, and 70 mM NaCl) for 2 min at 85 °C

followed by slow-cooling to room temperature and incubating overnight at –80 °C.

RNA-Binding Gel Shift Assays. Peptide and RNA were incubated together for 30 min on ice in 10 μ L binding reaction mixtures containing 10 mM HEPES–KOH, pH 7.5, 100 mM KCl, 1 mM MgCl₂, 0.5 mM EDTA, 1 mM dithiothreitol, 50 μ g/mL *E. coli* tRNA, and 10% glycerol. To determine relative binding affinities, 0.2 nM radiolabeled TAR RNA was titrated with increasing peptide concentrations, typically 1–128 nM for high-affinity TARs and 64–8192 nM for low-affinity TARs. RNA–peptide complexes were resolved on 10% polyacrylamide/0.5 \times TBE (45 mM Tris, pH 8.0, 45 mM boric acid, 1 mM EDTA) gels prerun for 1 h and allowed to cool to 4 °C. Gels were electrophoresed at 200 V for 2.5 h at 4 °C, dried, and autoradiographed or exposed to a phosphorimaging screen. For each TAR, the peptide concentration at which 50% of the total RNA was shifted into the complex, as determined visually from autoradiograms or phosphorimaging data, was used to estimate the apparent K_d (20). None of the RNAs examined showed unusual gel mobilities or binding behavior, suggesting that the 50% point provides a reasonable estimate of the apparent K_d . All values are expressed as affinities relative to wild-type BIV TAR [$100 \times K_d(\text{wt})/K_d(\text{mut})$].

Construction of Plasmids and β -Galactosidase Assays. TAR reporter plasmids were constructed by cloning synthetic oligonucleotide cassettes into an HIV LTR–LacZ reporter plasmid. The parent plasmid is derived from pcDNA3 (Invitrogen) and contains a modified HIV LTR in which restriction sites were placed on both sides of the TAR site for cloning of TAR mutants. The LacZ gene was cloned downstream of the HIV LTR using an EMC IRES–LacZ cassette (23). HIV Tat (residues 1–72) was expressed using pSV2tat72 (24), and Tat–BIV_{65–81}, which contains the HIV activation domain (residues 1–48) fused to the BIV arginine-rich domain (BIV Tat residues 65–81), has been described (20). Reporter plasmids and Tat–BIV_{65–81} or Tat_{1–72} plasmids were transfected into HeLa (human) or NIH 3T3 (murine) cells, and β -galactosidase activity was assayed after 44 h. For HeLa cell transfections, 1 μ g of reporter plasmid, 1 μ g of Tat plasmid, and 5 μ L of Lipofectin were incubated with cells in 3.8 cm² wells for 4 h using the recommended conditions (Life Technologies). Similar results were obtained using lower plasmid amounts (100 ng of reporter plasmid and 50 ng of Tat plasmid) along with pUC19 carrier DNA. For NIH 3T3 transfections, 500 ng of reporter plasmid, 500 ng of Tat plasmid, and 4 μ L of Lipofectamine were incubated with cells for 5 h. Cell extracts were assayed for β -galactosidase activity using ONPG for 0.1–2 h (25), and activities were normalized to the wild-type BIV TAR reporter.

RESULTS

HIV and BIV TAR Structures Are Similar. Given that HIV TAR has all the known sequence determinants for recognition by BIV Tat (Figure 1), we first asked whether the known NMR structures revealed any obvious differences in the arrangement of the required bases. We superimposed the bases in the BIV Tat binding site common to the two structures (Figure 2), and found that the position and orientation of each was well conserved, except for the bulge

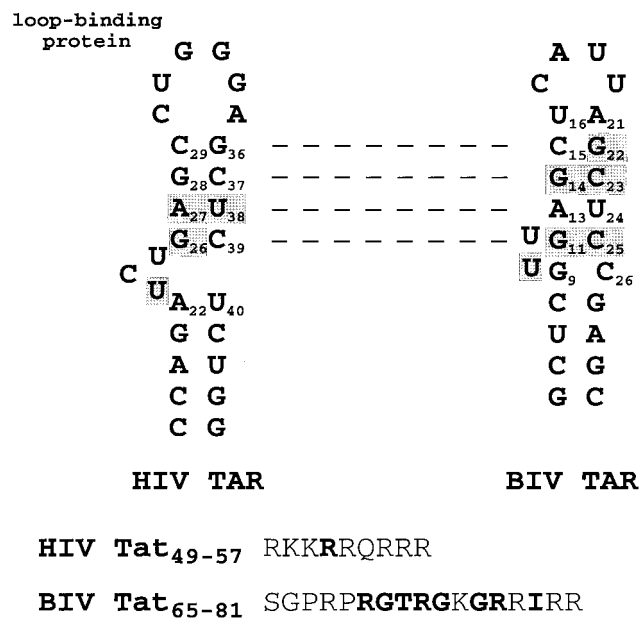


FIGURE 1: Comparison of HIV and BIV TAR RNAs and Tat arginine-rich RNA-binding domains. Nucleotides in each TAR important for binding by the cognate protein (20, 34) are highlighted, and sequence identity in the upper stems is indicated by dashed lines. The arginine-rich domains of the Tat proteins are shown, with amino acids important for RNA binding (9, 21) indicated in boldface type.

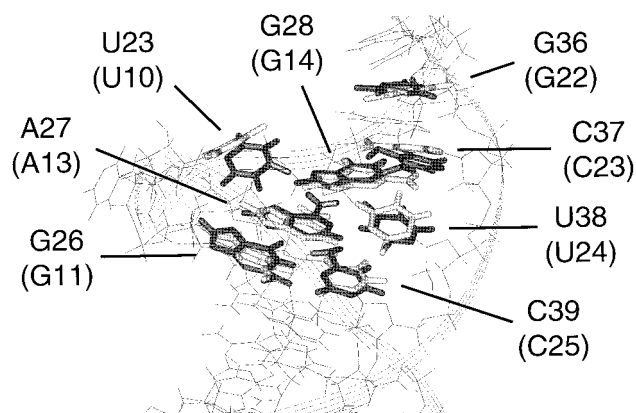


FIGURE 2: Superimposition of the two TAR structures. NMR models of the RNA components of the HIV-1 TAR-argininamide (11) and BIV Tat peptide-TAR complexes (4) were aligned using all bases known to be important for binding as well as the central A:U base pair (see Figure 1), but excluding the bulged uridine which is poorly fixed by the NMR data. Numbering refers to nucleotides in HIV TAR or BIV TAR (parentheses); the putative base triple is formed by U23 and the A27:U38 base pair in HIV TAR, and G26 is contacted by the arginine guanidinium group. The structure shown is the average calculated model of BIV TAR, with important bases highlighted in light gray and the corresponding bases of HIV TAR in dark gray.

uracil (U10 in BIV and the equivalent U23 in HIV). A bulge at this position is critical for BIV Tat recognition, and U10 has been proposed to participate in a base triple interaction analogous to that in HIV TAR (5); however, the positioning of U10 (or U23 in HIV) may be somewhat dynamic (3-5, 26), and mutagenesis data indicate that disrupting the putative base triple interaction has little effect on BIV peptide binding (20). The structural comparison (Figure 2) provided no obvious reason BIV Tat should not recognize HIV TAR,

though it did indicate that the bulge region, rather than the flanking base pairs which are recognized by BIV Tat, seemed most different between the two structures. The secondary structures (Figure 1) also show clear differences in the bulge regions, as well as sequence differences in the loop and lower stem. Thus, determinants in the bulge, loop, and/or lower stem must be responsible for the inability of BIV Tat to recognize HIV TAR.

The HIV Bulge Improves BIV Tat Binding. We suspected that differences in the bulge would be a major factor in determining binding specificity because the three-nucleotide HIV bulge is expected to destabilize coaxial stacking of the stems more than the two single-nucleotide BIV bulges (27). Indeed, NMR experiments show that the HIV stems are unstacked in the absence of peptide and become stacked upon binding (3, 11), whereas the BIV stems are stacked prior to binding (4, 5). It seemed reasonable that the BIV peptide might require a stable, preformed binding site in order to adopt its β -hairpin conformation. Thus, we expected that changing the bulge in BIV TAR to the three-nucleotide HIV bulge would decrease BIV peptide-binding affinity whereas changing the bulge in HIV TAR to the BIV configuration would increase affinity. In fact, the opposite result was obtained.

For all experiments described in this paper, we monitored RNA binding both in vivo and in vitro. For in vivo measurements, we constructed a series of HIV LTR reporters containing appropriate mutant RNAs in place of HIV TAR and measured transcriptional activation by Tat-BIV₆₅₋₈₁ (the HIV Tat activation domain fused to the BIV Tat RNA-binding domain) using a downstream LacZ reporter. β -Galactosidase activity is proportional to the relative RNA-binding affinity for each TAR variant. Because several TAR mutants have AUG sequences that might act as translational initiation sites upstream of LacZ, an encephalomyocarditis (EMC) virus internal ribosome entry site (IRES) was placed upstream of LacZ (23). For in vitro measurements, binding constants were determined using gel shift assays. Secondary structures of all RNAs were examined by computer folding (28) and no alternative forms were predicted.

Activation of the wild-type HIV TAR reporter by Tat-BIV₆₅₋₈₁ was ~7% that of BIV TAR (Figure 3), similar to that previously reported (20). Surprisingly, placing the HIV bulge into BIV TAR (B1) increased activity to ~70%. Conversely, placing the BIV bulge into HIV TAR (B2) decreased activity. To further probe the effect of the bulge, we tested BIV TARs containing bulges with one (B3) or two (B4) uridines. The single-nucleotide bulge decreased activity whereas the two-nucleotide bulge showed even greater activity than wild-type BIV TAR (Figure 3). Thus, BIV Tat does not appear to discriminate against HIV TAR based on the bulge, and indeed may even prefer an HIV configuration.

To ensure that the activities measured in vivo accurately reflect RNA-binding affinities, we performed gel shift experiments with a synthetic BIV Tat peptide (BIV Tat₆₅₋₈₁). The in vitro and in vivo results qualitatively agree quite well (Figure 3). In vitro, the BIV peptide binds with ~128-fold higher affinity to BIV TAR than to HIV TAR, and in vivo, an ~14-fold difference is observed. The intermediate binders show proportional affinity differences. It seems plausible that the difference in relative magnitudes reflects differences

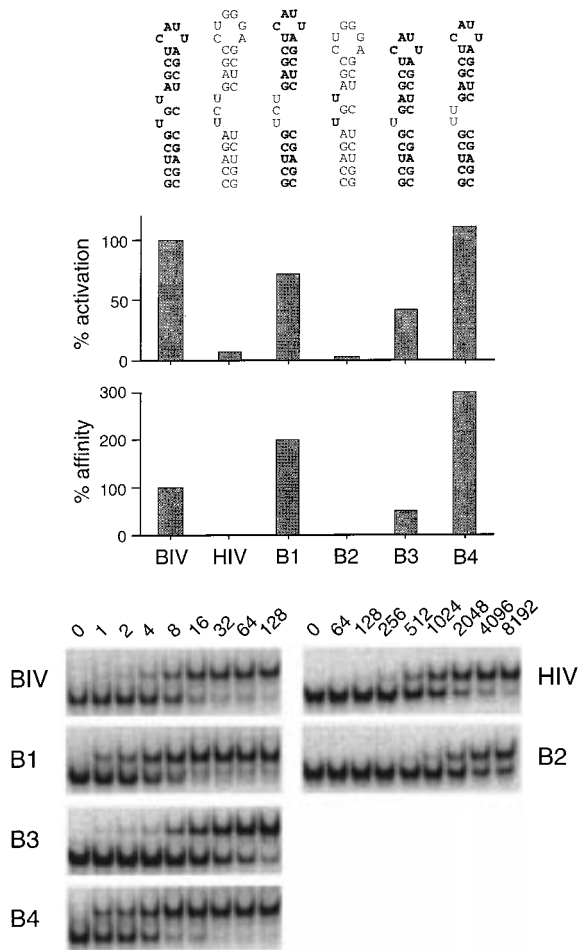


FIGURE 3: Activation of bulge hybrids by Tat-BIV₆₅₋₈₁ in vivo and RNA-binding affinities of BIV Tat₆₅₋₈₁ in vitro. BIV sequences are shown in boldface type and HIV sequences in plain text. Activation is plotted as a percentage of wild-type BIV TAR activity (upper graph), and RNA-binding affinity (determined from the representative gel shift data shown) is plotted as a percentage of wild-type BIV TAR binding affinity (lower graph).

in binding conditions (i.e., 4 °C versus 37 °C, the binding of other proteins, etc.). As in vivo, BIV TAR containing a two-nucleotide bulge (B4) bound most tightly, with ~3-fold higher affinity than wild-type BIV TAR. Thus, rather than destabilizing the binding site as we had suspected, a larger bulge actually appears to aid binding, perhaps by creating a less constrained TAR conformation or increasing major groove accessibility.

The HIV Stem Reduces BIV Tat Binding. Given that the bulge did not account for the inability of BIV Tat to recognize HIV TAR, we next examined the effect of nucleotide replacements in the lower stem. Previous biochemical studies showed that mutating the G9:C26 base pair immediately below the bulge, or the lower three base pairs, decreased binding affinity by <3-fold (20), suggesting that the lower stem did not contribute substantially to binding. However, the NMR experiments of Ye et al. (7) showed an NOE between Arg77, an essential amino acid, and G9, suggesting a possible contact that would be unlikely to occur with the A:U pair of HIV TAR.

When the BIV TAR lower stem was replaced with the HIV stem (S1), activation was reduced to ~14% of wild-type BIV TAR (Figure 4). Conversely, when the lower stem of HIV TAR was replaced with the BIV stem (S2), activation

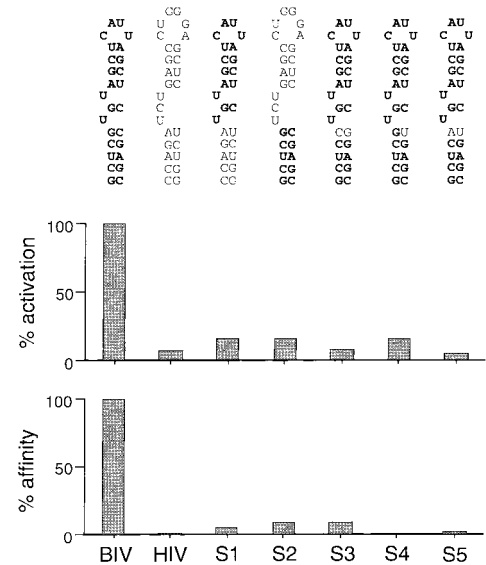


FIGURE 4: Activation of lower stem hybrids by Tat-BIV₆₅₋₈₁ in vivo and RNA-binding affinities of BIV Tat₆₅₋₈₁ in vitro. BIV sequences are shown in boldface type and HIV or mutant sequences in plain text. Activation is plotted as a percentage of wild-type BIV TAR activity (upper graph), and RNA-binding affinity is plotted as a percentage of wild-type BIV TAR binding affinity (lower graph).

increased 2–3-fold relative to HIV TAR. Thus, the lower stem of HIV TAR appears to significantly weaken BIV Tat binding. Mutating the G9:C26 base pair alone to C:G (S3) reduced activity to ~9% (a somewhat greater effect than observed previously; ref 20), mutating the base pair to G:U (S4) reduced activity to ~16%, and mutating the base pair to A:U (S5) reduced activity to ~5%. In vitro binding affinities correlated well with the in vivo results, except that the G9:U26 mutant (S4) bound even more weakly than HIV TAR (Figure 4). These results suggest that the nature of the terminal base pair is important, either because it provides a contact to the peptide, clamps the lower helix shut, changes the major groove width, and/or provides important stacking interactions with the bulge and upper stem. Additional base pairs below the clamping pair may further modulate the interaction; for example, S5 differs from S1 only in the three base pairs below G9:C26, but binding of S5 is ~3-fold weaker.

The Loop Region Is Important for BIV Tat Binding. Previous experiments have shown that the sequence of the BIV TAR loop is not important for peptide binding (20). Nevertheless, the BIV TAR loop region does not simply differ in sequence from HIV but rather contains a four-nucleotide loop and a U16:A21 base pair in place of a six-nucleotide loop (Figure 1). It has been reported that the HIV loop may adopt an unusual structure (29–31), and it seemed plausible that such a structure might block access to the binding site or that the additional base pair might be important for BIV Tat recognition. Replacing the entire six-nucleotide BIV TAR loop region (the loop and top base pair) with the six-nucleotide HIV loop (L1) decreased activity to ~10% (Figure 5). Conversely, replacing the HIV loop with the BIV loop region (L2) slightly increased activity relative to HIV TAR. Thus, the HIV TAR loop appears to significantly inhibit binding of BIV Tat.

Replacing the four-nucleotide loop of BIV TAR with the equivalent four nucleotides from HIV TAR (L3) had little

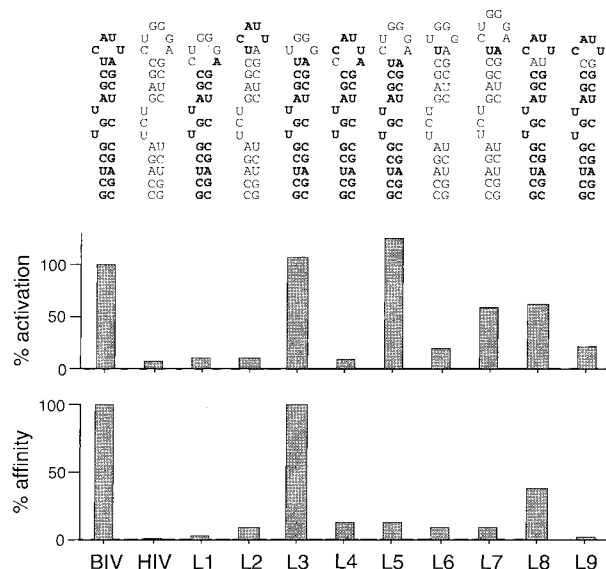


FIGURE 5: Activation of loop hybrids by Tat-BIV₆₅₋₈₁ in vivo and RNA-binding affinities of BIV Tat₆₅₋₈₁ in vitro. BIV sequences are shown in boldface type and HIV or mutant sequences in plain text. Activation is plotted as a percentage of wild-type BIV TAR activity (upper graph), and RNA-binding affinity is plotted as a percentage of wild-type BIV TAR binding affinity (lower graph).

effect on activation, whereas mutating the U16:A21 base pair to the C:A mismatch of HIV (L4) strongly decreased activation (Figure 5). Replacing the four-nucleotide loop with the entire six-nucleotide HIV loop, but preserving the U16:A21 pair (L5), resulted in a TAR more active than wild-type BIV TAR. In the context of HIV TAR, a U:A pair in place of C:A (L6), or with an additional U:A pair (L7), increased activity from ~7% to ~20–60%. The precise nature of the top base pair affects activity; mutating U16:A21 of BIV TAR to A:U (L8) gave ~62% activity whereas mutating to C:G (L9) gave ~21% activity. The results clearly suggest that the absence of a clamping base pair between the peptide-binding site and the HIV TAR loop accounts for much of the RNA-binding discrimination.

In vitro binding affinities of loop variants revealed a similar pattern (Figure 5), with two interesting exceptions. In both the BIV and HIV TAR contexts, a closing U:A base pair together with the entire six-nucleotide HIV loop (L5 and L7) supported strong activation, but both TARs showed poor binding in vitro. The reason for the discrepancy is unclear, but it seems plausible that the HIV loop structure is stable at 4 °C and thereby interferes with binding in vitro whereas the structure may be unstable at 37 °C in vivo.

The Loop Binding Factor Does Not Interfere with BIV Tat Binding. In a current model of HIV Tat-mediated activation, the arginine-rich domain of Tat binds to the TAR bulge and a host protein interacts with the TAR loop, and presumably with Tat, to stabilize the complex. To examine whether the loop factor might interfere with, or possibly assist, the binding of BIV Tat, we measured activities of HIV TAR reporters in a murine cell line (NIH 3T3) believed to lack the factor (13–15). In general, there is excellent agreement between the results in human and murine cells (Figure 6), though the activity of an HIV TAR containing a U:A pair inserted below the loop (L7) is much higher in human than in mouse cells. The behavior of L7 may indicate that the loop factor assists binding in this case, and may account for

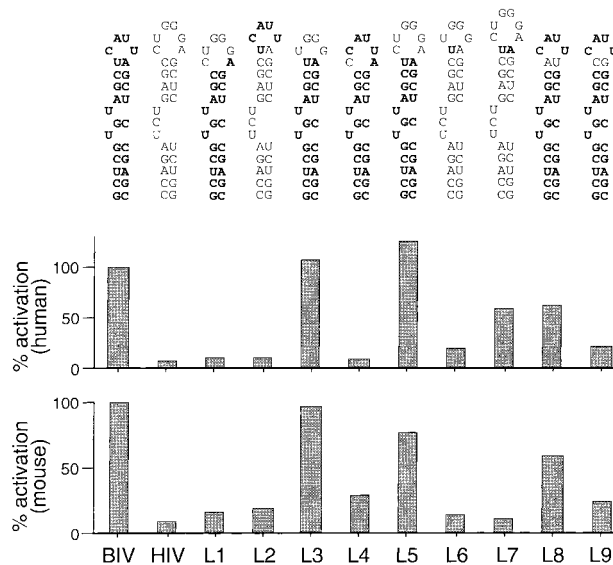


FIGURE 6: Activation of loop hybrids by Tat-BIV₆₅₋₈₁ in human (upper graph) and mouse (lower graph) cells. BIV sequences are shown in boldface type and HIV or mutant sequences in plain text. Activation is plotted as a percentage of wild-type BIV TAR activity.

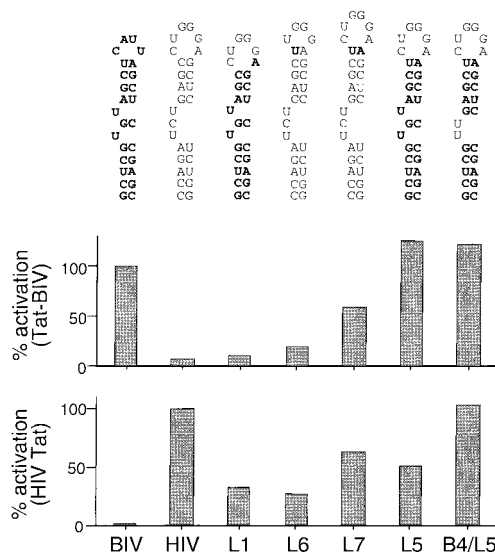


FIGURE 7: Activation of bifunctional TARs in vivo. BIV sequences are shown in boldface type and HIV sequences in plain text. Activation is plotted as a percentage of activity of Tat-BIV₆₅₋₈₁ on wild-type BIV TAR (upper graph) or HIV Tat on wild-type HIV TAR (lower graph).

the difference between the in vivo and in vitro results described above. In general, the results suggest that the loop factor does not inhibit BIV Tat binding, but rather may assist binding to some HIV loop variants.

Bifunctional TARs. In exploring the specificity of BIV Tat binding, it appeared that the structural requirements for activation by HIV or BIV Tat could be met simultaneously in the same TAR molecule. We tested some likely bifunctional reporters for activation by both proteins (Figure 7), and, indeed, found that adding an HIV loop to BIV TAR (L1, L5), or a U:A base pair to HIV TAR (L6, L7), increased activation by the noncognate Tat. The results from other mutants described above indicate that BIV Tat prefers a BIV TAR stem, a two-nucleotide bulge, and a U16:A21 base pair, and it is known that HIV Tat requires a six-nucleotide HIV TAR loop and a bulge of at least two nucleotides. Because

each Tat can tolerate the optimal requirements for the other, we constructed a hybrid containing all essential features for both proteins and measured activation. Indeed, the hybrid reporter (B4/L5) was strongly activated by both HIV and BIV Tat, suggesting that a single TAR can efficiently adopt both HIV and BIV Tat binding strategies.

DISCUSSION

We have shown that the BIV Tat arginine-rich domain effectively discriminates between BIV and HIV TAR sites through subtle differences in the regions flanking the peptide-binding site. The larger bulge of HIV TAR does not interfere with recognition, but rather the lack of a clamping base pair above the binding site and sequence differences in the lower stem account for poor binding to HIV TAR. We also have shown that the putative HIV TAR loop binding protein neither significantly assists nor inhibits BIV Tat activation of HIV TAR *in vivo*. Based on these results, we designed a hybrid TAR that is activated efficiently by both BIV Tat and HIV Tat.

We initially suspected that the HIV bulge would be responsible for poor recognition by BIV Tat. Larger bulges, such as the three-nucleotide bulge in HIV TAR, are expected to disrupt coaxial stacking of the stems (27), and because BIV peptide folding is coupled to binding, it seemed plausible that a preformed binding site might be required for high-affinity binding. Contrary to our expectation, the HIV bulge was well tolerated *in vivo* and in fact increased BIV peptide affinity *in vitro*. A BIV TAR containing a variant HIV two-nucleotide bulge displayed even tighter binding than wild-type BIV TAR, suggesting that the larger bulge provides a more favorable conformation, perhaps by widening the major groove or allowing more flexibility to the site. A two-nucleotide bulge also is preferred in HIV TAR (32).

Features of both the upper and lower stems account for the specificity of BIV Tat binding. The presence of a base pair above the binding site is critical for binding and likely acts as a clamp to prevent fraying of the site. The marked preference for U:A or A:U pairs suggests a subtle role of RNA structure, perhaps related to RNA stability or stacking of the loop on the upper stem. In the lower stem, the HIV sequence is poorly tolerated, in part because the clamping pair below the binding site is a less stable A:U pair; indeed, a G:C pair at this position in HIV TAR is known to improve HIV Tat binding (33). It also has been proposed that G9 may directly contact Arg77 based on NMR (5) and footprinting (20) data, though previous mutagenesis experiments suggested relatively few sequence requirements in the lower stem (20). The results presented here indicate a distinct preference for the wild-type BIV stem over others tested and also indicate that the HIV stem is particularly poor. Again, a relatively subtle feature of the stem sequence, perhaps related to stacking of the stem against the lower part of the binding site or stability of the structure, probably accounts for the specificity and may influence a possible contact to Arg77. Alternatively, the HIV sequence, or other sequences, might contain antideterminants to binding.

The HIV loop was found to significantly decrease BIV Tat binding affinity *in vitro* but not *in vivo*, perhaps because a stable loop structure can form and block binding at 4 °C

but not at 37 °C. Evidence for loop structure comes from footprinting experiments at low temperature (29, 30); subsequent NMR studies at room temperature indicate a relatively flexible loop with modest structure (3, 31). In this study, we focused on why BIV Tat does not recognize HIV TAR in the same manner as it recognizes BIV TAR even though all nucleotide determinants appear to be present. In principle, it was possible that BIV Tat would use the HIV loop binding protein to increase affinity for HIV TAR *in vivo*, perhaps also utilizing BIV-like interactions with the RNA. In general, this does not seem to be the case, however, because strong activation is observed in mouse cells lacking the factor. One variant with a suboptimal lower stem (L7) displays higher activity in human than in mouse cells, suggesting that the loop factor may help stabilize the Tat–TAR complex in this case.

The similarities in structure between HIV and BIV TAR raise the question of whether these RNAs might have evolved from a common viral ancestor capable of using both the BIV- and HIV-binding modes. We have shown that it is possible to create bifunctional TARs that can be activated efficiently by both HIV and BIV Tat, providing one possible route to evolve distinct specificities from a primordial RNA. In essence, specificity can arise passively through selection of TAR mutants able to bind one Tat protein while simultaneously losing affinity for others. It seems quite remarkable that such high discrimination can be achieved by short peptides, even for distinctly similar RNA structures, yet it is becoming increasingly apparent that many recognition strategies are possible even for such small complexes.

ACKNOWLEDGMENT

We thank Cynthia Honchell for peptide and oligonucleotide synthesis, and Donna Campisi and Kazuo Harada for comments on the manuscript.

REFERENCES

1. Tan, R., Chen, L., Buettner, J. A., Hudson, D., and Frankel, A. D. (1993) *Cell* 73, 1031–1040.
2. Tan, R., and Frankel, A. D. (1995) *Proc. Natl. Acad. Sci. U.S.A.* 92, 5282–5286.
3. Aboul-ela, F., Karn, J., and Varani, G. (1995) *J. Mol. Biol.* 253, 313–332.
4. Puglisi, J. D., Chen, L., Blanchard, S., and Frankel, A. D. (1995) *Science* 270, 1200–1203.
5. Ye, X., Kumar, R. A., and Patel, D. J. (1995) *Chem. Biol.* 2, 827–840.
6. Battiste, J. L., Mao, H., Rao, N. S., Tan, R., Muhandiram, D. R., Kay, L. E., Frankel, A. D., and Williamson, J. R. (1996) *Science* 273, 1547–1551.
7. Ye, X., Gorin, A., Ellington, A. D., and Patel, D. J. (1996) *Nat. Struct. Biol.* 3, 1026–1033.
8. Su, L., Radek, J. T., Hallenga, K., Hermanto, P., Chan, G., Labeots, L. A., and Weiss, M. A. (1997) *Biochemistry* 36, 12722–12732.
9. Calnan, B. J., Tidor, B., Biancalana, S., Hudson, D., and Frankel, A. D. (1991) *Science* 252, 1167–1171.
10. Tao, J., and Frankel, A. D. (1993) *Proc. Natl. Acad. Sci. U.S.A.* 90, 1571–1575.
11. Puglisi, J. D., Tan, R., Calnan, B. J., Frankel, A. D., and Williamson, J. R. (1992) *Science* 257, 76–80.
12. Calnan, B. J., Biancalana, S., Hudson, D., and Frankel, A. D. (1991) *Genes Dev.* 5, 201–210.

13. Hart, C. E., Galphin, J. C., Westhafer, M. A., and Schochetman, G. (1993) *J. Virol.* 67, 5020–5024.
14. Alonso, A., Cujec, T. P., and Peterlin, B. M. (1994) *J. Virol.* 68, 6505–6513.
15. Wei, P., Garber, M. E., Fang, S.-M., Fischer, W. H., and Jones, K. A. (1998) *Cell* 92, 451–462.
16. Berkhout, B., and Jeang, K. T. (1991) *Nucleic Acids Res.* 19, 6169–6176.
17. Luo, Y., and Peterlin, B. M. (1993) *J. Virol.* 67, 3441–3445.
18. Luo, Y., Madore, S. J., Parslow, T. G., Cullen, B. R., and Peterlin, B. M. (1993) *J. Virol.* 67, 5617–5622.
19. Newstein, M., Lee, I. S., Venturini, D. S., and Shank, P. R. (1993) *Virology* 197, 825–828.
20. Chen, L., and Frankel, A. D. (1994) *Biochemistry* 33, 2708–2715.
21. Chen, L., and Frankel, A. D. (1995) *Proc. Natl. Acad. Sci. U.S.A.* 92, 5077–5081.
22. Milligan, J. F., and Uhlenbeck, O. C. (1989) *Methods Enzymol.* 180, 51–62.
23. Ghattas, I. R., Sanes, J. R., and Majors, J. E. (1991) *Mol. Cell. Biol.* 11, 6438–6459.
24. Frankel, A. D., and Pabo, C. O. (1988) *Cell* 55, 1189–1193.
25. Sambrook, J., Fritsch, E. F., and Maniatis, T. (1989) *Molecular Cloning: A Laboratory Manual*, Cold Spring Harbor Laboratory Press, Cold Spring Harbor, NY.
26. Brodsky, A. S., and Williamson, J. R. (1997) *J. Mol. Biol.* 267, 624–639.
27. Weeks, K. M., and Crothers, D. M. (1993) *Science* 261, 1574–1577.
28. Zuker, M. (1989) *Science* 244, 48–52.
29. Colvin, R. A., and Garcia-Blanco, M. A. (1992) *J. Virol.* 66, 930–935.
30. Colvin, R. A., White, S. W., Garcia-Blanco, M. A., and Hoffman, D. W. (1993) *Biochemistry* 32, 1105–1112.
31. Jaeger, J. A., and Tinoco, I., Jr. (1993) *Biochemistry* 32, 12522–12530.
32. Weeks, K. M., and Crothers, D. M. (1991) *Cell* 66, 577–588.
33. Tao, J., and Frankel, A. D. (1996) *Biochemistry* 35, 2229–2238.
34. Hamy, F., Asseline, U., Grasby, J., Iwai, S., Pritchard, C., Slim, G., Butler, P. J., Karn, J., and Gait, M. J. (1993) *J. Mol. Biol.* 230, 111–123.

BI980382+